A 14-day Dexamethasone timecourse exposure in Caco-2 monolayers results in differential expression of tight-junction and cytoskeleton regulatory pathway genes

Robinson, J.M.[1], Abey, S.A.[1*], Kenea, N.D.[1*], Henderson, W.A.[1,2]
1. Digestive Disorder Unit, Biobehavioral Branch, Division of Intramural Research, National Institute of Nursing Research (NINR), National Institutes of Health (NIH), Department of Health and Human Services (DHHS), Bethesda, MD, USA.
2. Henderson OrcidID: 0000-0003-3924-7118, Scopus Author ID: 32367603100

* See current address information in Acknowledgements section

Contact:
Dr. Jeffrey M. Robinson
jeff.robinson.evol@gmail.com
301-335-4851

Abstract:
Glucocorticoid (GC) hormones are modulators of endogenous stress responses and are important pharmaceuticals for inflammatory and autoimmune diseases. The gastrointestinal epithelium is a significant tissue target of Glucocorticoids; perturbation of epithelial barrier function during the endogenous stress response plays a major role in the pathophysiology of inflammatory bowel disease. Epithelial permeability and barrier function are mediated by the tight junction protein complex, with a network of molecular/cellular interactions occurring between the actin cytoskeleton, RhoGTPase, Akt/PI3K and growth factor receptor, and inflammatory cytokine signaling, influencing the establishment of a 'partial EMT' phenotype. To improve our understanding of GC-responsive gene expression in a gastrointestinal epithelial context, we tested polarized Caco-2 monolayer cultures during at 30-day timecourse, with 15-days of continuous Dexamethasone exposure. Trans-epithelial resistance (TEER) was recorded to provide a physiological quantification of barrier function during the timecourse treatments. Presence of intracellular glucocorticoid hormone activates the human glucocorticoid receptor (GCR, human NR3C1 gene) transcription factor, resulting in transcriptional activation and repression of various GCR-responsive genes. We tested for differential gene expression with a multiplexed panel of 250 gene expression panel using the Nanostring nCounter® system. Gene panel selection was based on membership of genes in canonical KEGG pathways for tight-junction, adherens junction, focal adhesion, actin cytoskeleton regulation, and colorectal cancer. Our TEER results confirm, as previously reported, that long-term Dexamethasone exposure results in decreased permeability in Caco-2 monolayers ~day 20-25. Culture age and Dexamethasone exposure both contributed to differential gene expression for cell-cell junction, protein kinases, survival and cancer- associated genes, reported here in the context of their corresponding KEGG pathway representations. The findings give evidence for GC- and time-associated patterns of transcriptional response and provide further insight into long-term glucocorticoid-associated physiological effects on the gastrointestinal epithelia. Future research utilizing more advanced cell culture methods will use this data-set as a reference.

Keywords: intestinal epithelial barrier, enterocyte, tight junction, actin cytoskeleton, Caco-2, glucocorticoid, Dexamethasone, KEGG Pathway Database, NanoString Technologies®, nSolver, nCounter, trans-epithelial resistance, TEER.

Abbreviations: Glucocorticoids (GCs), Glucocorticoid Receptor (GR, geneID hsNR3C1), Glucocorticoid Response Elements (GREs), Occludin (OCLN), Zona Occludans-1 (TJP, ZO-1), Dexamethasone (DEX), Colorectal Cancer (CRC), Tight Junction (TJ), Intestinal Epithelial Cells (IECs), Adherens Junction (AJ), Trans-epithelial (electrical) resistance (TEER), Kyoto Encyclopedia of Genes and Genomes (KEGG), False Discovery Rate-corrected (FDR).

Introduction

Glucocorticoids (GCs) facilitate physiological stress response in tissues throughout the body. Stressors may include inflammation resulting from infection or tissue damage, hypoglycemia, physical pain, and perceived psychological stress (Kadmiel and Cidlowski, 2013). Inflammation and other stressors are associated with perturbations of gastrointestinal barrier function (Soderholm and Perdue, 2001). The anti-inflammatory, immunosuppressive effects of GCs make them important pharmacological agents against chronic disorders including inflammatory bowel disease, arthritis, asthma, and others (Buttgereit et al, 2005; Cain and Cidlowski, 2017). Long-term negative side effects of use are also recognized (Coutinho and Chapman, 2011). GCs bind and activate the Glucocorticoid Receptor (GCR, gene NR3C1) transcription factor, resulting in transcriptional gene regulation. In inflammatory-regulating cells such as macrophages (Gupte et al, 2013; Uhlenhaut et al., 2013), GCR activates anti-inflammatory genes and suppresses pro-inflammatory genes in conjunction with STAT transcription factors in the TGF-B pathway (Petta et al, 2016; Xavier et al, 2016).

Reports of transcriptional effects of GC gene activation in enterocyte and colonocyte cell-type specific models are limited. In GI epithelia, barrier dysfunction results from inflammatory-immune signaling, however effects resulting from GCR transcriptional regulation, such as is seen in respiratory epithelium (Gerber, 2015; Vockley, 2016), are not well known. Barrier function is dependent on the tight-junction (TJ) complex, the actin cytoskeleton, and Rho GTPase signaling pathways (Bruewer et al, 2004; Citi et al, 2014). These pathways interact to establish and maintain epithelial integrity and identity and modulate barrier function associated with gastrointestinal pathophysiology (Krug et al, 2014; Lee, 2014). To improve resolution of GC-induced transcriptional effects on these pathways in GI epithelia-specific context, we exposed colonocyte-like polarized monolayers of the Caco-2 cell line to the synthetic, long-acting glucocorticoid Dexamethasone (DEX) for 25 days. We measured differential gene expression using the Nanostring® nCounter system (Geiss et al, 2008), using a panel of 250 genes from canonical KEGG pathways of interest (Kanehisa et al, 2000; Robinson and Henderson, 2018). Changes in barrier function over time and from DEX exposure were recorded using trans-epithelial resistance (TEER). Student's T-tests for differential gene expression based on culture timepoint and DEX exposure were performed, with false discovery rate correction, to show contributions from each variable to expression of selected cell-cell junction genes, protein kinases, survival and cancer- associated genes.

The tight junction mediates epithelial barrier function in cooperation with RhoGTPase pathways.

Extracellular domains of trans-membrane Occludin (OCLN) and Claudin family proteins mediate the barrier function of the TJ through intercellular dimerization, forming a cell-cell junctional component of the meshwork infrastructure of the epithelial membrane (Zihni et al, 2016; Fig. 1A). Occludin blocks paracellular translocation of macromolecules, while Claudin family members provide selective permeability to small ionic molecules (Krug et al, 2014). Expression of Claudins have been shown to be affected by Dexamethasone exposure in Caco-2 cell culture (Fischer et al, 2014). Zona Occludens, ZO-1 (TJP) protein provides a hub between the transmembrane proteins and filaments of the actin cytoskeleton. The TJ is described as the 'zonular signalsome' because of extensive crosstalk between TJ, AJ, and RhoGTPase signaling (Gonzalez-Mariscal et al, 2008; Dorfel and Huber, 2012; Schneeberger and Lynch, 2004; Turner et al, 2014).

RhoGTPase signaling is important in establishing and maintaining epithelial polarity and homeostasis (22), and plays a key role in EMT (Mack and Georgiou, 2014; Quiros and Nusrat, 2014). Actin cytoskeletal dynamics are highly regulated via signaling from the Rho GTPase family members RhoA, Rac1 and Cdc42, which control actin polymerization through regulation of the WAVE, WASP, Arp2/3 complex (Appenstrom, 1999; Bruewer et al, 2004; Burridge and Wennerberg, 2004; Fig. 1C). Rho-family GTPases exert specific regulatory effects on TJ transmembrane proteins (Bruewer et al, 2004), and TJ proteins provide active feedback into the Rho GTPase pathway (Citi et al, 2014).

Glucocorticoid mechanisms of transcriptional regulation.

GC-activation causes GCR dimerization, nuclear localization and binding to promotor/enhancer-associated DNA

sequence (described as "glucocorticoid responsive elements" (GREs)). In genome-level studies investigating GRE-binding and transcriptional activation in DEX-treated lung epithelial cell cultures (Vockley et al, 2016), and in DEX-treated, LPS-activated macrophages (Chinenov et al, 2014; Gupte et al, 2013), it has been demonstrated that significant combinatorial interactions occur between GCR and other transcription factors to provide contextual specificity for the transcriptional response.

Experimental Approach and Rationale.

A multiplexed gene-expression panel strategy gives us better understanding of gene expression patterns affecting epithelial barrier function in Caco-2 cells, identify putative binding-sequence motifs, while partially addressing the following aspects of GC-associated questions:

1. Long-term GC exposure. Studies investigating DEX-responsive differential gene expression are commonly limited to short timecourse studies (hours). Our 25-day Dex exposure experiment represents a lengthy aging interval for an epithelial layer with better resolution of longer-term responses.
2. Intestinal epithelial cell-type specificity. Effects of DEX treatment from a transcriptomics point-of-view have primarily been reported for immune cells (Macrophages and T-cells), or in airway epithelia. Here we focus on the classical Caco-2 colon epithelial cell culture system.
3. Pathway specificity. Determination of how co-regulatory motifs affect pathway-specific physiological functions from transcriptomics datasets remains difficult due to the high complexity of whole-transcriptome regulatory interactions. Use of subset, pathway-specific gene expression panels provide a focused approach, in this case, specific to epithelial barrier function-associated pathways of interest.

Methods

Caco-2 cell culture and trans-epithelial resistance (TEER).

Caco-2 colorectal adenocarcinoma-derived cell line used, purchased from American Type Culture Collection (ATCC# HTB-37). Seeded Caco-2 cells differentiate into a polarized monolayer morphologically and physiologically similar to colon epithelia, with an expressed and functional tight-junction. The cell line has a decades-long history of use in pharmacokinetic assays for drug absorption and basic research on epithelial barrier function (Hidalgo et al, 1989; Natoli et al, 2012).

Cells were seeded onto 24-well insert plates with polyethylene terephthalate (PET) permeable membranes with 1.0 uM pore size (Millipore product # PSRP010). Seeding volume was 300uL cells at density of $.4x10^6$ cells/mL (or 120,000 cells/well) in the apical chamber, with 600uL media in the basolateral chamber. Cultures were thawed from cryopreserved vials with 5 or 6 previous passages. Cultures were grown in incubator at 37°C, 5% CO2 on filter-sterilized Eagle's Minimum Essential Medium (EMEM) with 20% Fetal Bovine Serum, with Penicillin-Streptomycin (Quality Biological™ cat. # 120-095-671). Cryovials were thawed, resuspended, and pelleted to remove DMSO and suspended in 12mL in T75 flasks. Adherent cells were grown to 60-80% confluency and split by aspirating media, rinsing with Hank's Buffered Salt Solution (HBSS), and harvesting with .25% Trypsin-EDTA. Live cell counts were obtained by adding 10uL cells to 10uL .4% Trypan Blue/ .85% NaCl (BioWhittaker® catalog# 17-942E) and counting on the Nexcelom Bioscience Cellomenter™ Auto T4. Media was changed every other day during the experiments.

Trans-epithelial resistance readings were taken at regular intervals during the experimental timecourse with the Millicell ERS-2 Epithelial Volt-Ohm Meter (cat. # MERS00002). Cell cultures were equilibrated to room-temperature (22°C) before readings were taken, in order to control for temperature effects on TEER readings (Blume et al., 2010).

Timecourse and DEX treatment.

Dexamethasone exposure was begun between 11-13 days post-seeding, after the epithelial monolayer became polarized and cell density was stable for 2-3 days (See Fig. 2B, Experimental timecourse). Dex was applied to experimental wells at 10uM. We used Sigma reagent D2915 "Dexamethasone-Water Soluble". Water-soluble

Dex is compounded with methyl-β-cyclodextrin, product documentation states the dry reagent is 65mg/g Dexamethasone by weight. Dex molecular weight was indicated 392.5g/mol. Stock was made by dissolving Dexamethasone-Water Soluble at 10 grams/L. 10uM Dex in media was obtained by using: 65mg/g x 10g/L = .65g/L x 1mol/392.5g = .00166mol/L = 1.66mM = 1660uM. For 10uM, added .06mL Dexamethasone-Water Soluble stock to 10mL media. Control cell cultures were grown in standard media without Dex or cyclodextrin carrier. As Dex is commonly orally administered in conjugated form, the treatment can be interpreted as a model for cellular action during pharmacokinetic exposure of conjugated Dex *per se*, rather than generalized to glucocorticoid-binding activity in general.

Total RNA was extracted from fresh monolayers at three timepoints during DEX treatment:
T1: 15-18 days post-seeding, at 2-3 days of DEX treatment.
T2: 23-25 days post-seeding with 10-13 DEX treatment.
T3: 30 days post-seeding with 18 days DEX treatment.

RNA Extraction.
Total RNA including small RNA from Caco-2 monolayers was extracted from individual permeable membrane inserts at the three experimental timepoints using the Qiagen miRNeasy® Micro kit (cat. #217084) with RNeasy® MinElute® spin columns (mat. #1026497). Extracted total RNA was quantified with Thermo Scientific™ NanoDrop™ spectrophotometer. RNA was stored at -80°C until assaying.

Experimental Replicates and Statistical Design.
We performed three separate, 30-day experimental 'runs', where we collected multiple RNA samples for three timepoints from Dex+ and Control-treated Caco-2 monolayers. Our statistical framework was conceived as a 2 x 3-timepoint design, however in the text we focus reporting on statistical comparisons between (Dex+/Control and T1/T3), while (T1/T2 showed similar, but smaller differential effects). In total, T1 had 4 Dex+ and 4 Control samples, T2 had 4 Dex+ and 6 Control samples, and T3 had 3 Dex+ and 2 Control samples (see Supplementary Results 1, Table1). Each sample represents RNA extracted from an individual well (ie. one permeable membrane support).

Nanostring expression profiling and Gene-panel selection.
We designed a 250-probe custom codeset for use with Nanostring Technologies™ methodology, which provides amplification-free molecular count data from a multiplexed, fluorescent barcode-conjugated oligonucleotide probe set. The Nanostring nCounter™ instrument provides automated sample processing with optical barcode counting (Geiss et al, 2008). Complete probe sequences and isoform coverage are reported in (Supplementary Methods 1.2, Codeset_probe_specifications); also see (Robinson and Henderson, 2018) for additional description of gene panel selection criteria.

Our panel selection strategy made use of KEGG pathway database (Kanehisa et al, 2000). We selected a panel of gene probes focused on intestinal-epithelial barrier function and pathology-associated pathways described above. Canonical KEGG pathways genes were selected from included tight-junction (map04530), regulation of actin cytoskeleton (map04810), colorectal cancer (map05210), selected for additional genes with significant overlapping membership in the adherens junction (map04520), focal adhesion (map04510), Wnt (map04310), and others (Table 1A, Supplementary Methods 1.1, Codeset Annotations). Genes not expressed in lower gastrointestinal tissues were excluded by referencing against the Human Protein Expression Atlas (which includes tissue-specific RNA expression) (Uhlen et al, 2015). Additional genes of interest were included on an ad hoc basis:

1. KEGG microRNA gene targets associated with colorectal cancer (map05206). These include Programmed cell death 4 (PDCD4), DNA methyltransferase 3A (DNMT3A), and others.
2. Core microRNA biogenesis pathway genes Drosha (RNASEN), Pasha (DGCR8), Dicer, Argonaute2, Exportin5, and the RISC loading complex RNA binding subunit (TRBP) to provide further understanding of potential

pan-miRNA processing effects.

3. Genes with observed exhibiting differential expression from our clinical cohort of IBS patients (Abey et al, 2016), including chemokine receptor CXCR4 and Lysozyme (LYZ) and others.
4. Enterocyte/colonocyte differentiation markers Carbonic anhydrase I and II (CAI, CA2) (Bekku et al, 1998), and cancer stem marker Aldehyde dehydrogenase 18, isoform A1 (Marcato et al, 2011) were included to provide additional indicator of cellular differentiation.
5. Additional genes with high specific expression in gastrointestinal tissue according to Human Protein Expression Atlas, including additional Claudins, heat shock proteins, and others.

Differential Expression Analysis and Data Visualizations with Nanostring nSolver™ software.
Differential expression statistical analyses, and other graphical readouts were performed with the the Nanostring nSolver™ v3.0 software (MAN-C0019-06, April 2016) and Advanced Analysis 1.1.5 Plugin (MAN-100300-01, August 2016). The software provides complete tools for differential expression statistical analyses of Nanostring probe count data.

Reference genes for normalization of read count data were obtained with geNorm algorithm (Vandesompele et al, 2002), in the R-language Bioconductor package NormqPCR (Perkins et al., 2012), implemented within Nanostring nSolver™ software. The geNorm algorithm selects reference probes based on global stability (M_i) of pairwise expression ratio between samples, iteratively identifying genes with the lease expression variance, we chose 10 genes with minimum M_i values as normalization reference genes. Raw count data, variance and geNorm reference gene selection data are provided (Supplementary Methods 1.3, MeanVariance_geNorm_RefGene).

Our differential expression analysis followed the best practices as outlined in the Nanostring Gene Expression Data Analysis Guidelines (MAN-C0011-04, 2017). Multivariate linear regression is used as a multivariate statistical method Nanostring Advanced Analysis 1.1.5 Plugin, providing a statistical model for correcting effects of the confounding variables (Nanostring MAN-100300-01, August 2016). During each statistical test, a confounder variable was assigned (ie. timecourse) for a predictor variable (ie. Dex treatment), and vice-versa.
P-values were generated with Benjamini-Yekutieli method for correcting false discovery rate (Benjamini and Yekutieli, 2001).

Results

Differential Expression associated with DEX and timepoint variables.
DEX enhances culture age-related transcriptional patterns in some genes, opposes age-associated trends in others, and has minimal effect on the majority of expressed genes. Co-expression analysis supports a set of epithelial-barrier associated genes with putative underlying GCR-responsiveness.
Results of DE analysis shows differentially expressed genes associated with each of the variables: DEX treatment and timecourse progression. (Table 1; Fig. 3A-DEX vs. Untreated, B-TP2 vs. TP1, C-TP3 vs. TP1; Supplementary Results 1.1-1.3; Supplementary Results 2. Raw probe counts).
Broadly, the results show relatively stable gene expression, with average positive DEX-associated fold change of .42, and average positive T3 vs. T1 fold change of 1.14 for genes with significant DE (BY p-value ≤ .05). Timecourse progression was associated with higher average fold changes: CXCR4 with a 5.0-fold change compared with DEX-associated 2.8-fold change increase for CXCR4. Negative fold changes were less common, with 7 out of 23 (30%) DEX-associated DE showing decreased expression, TP3vsTP1 showing 9 out of 22 (40%) with negative fold-change. TP-2 vs. TP-1 genes exhibited a similar but more moderate pattern of DE compared with TP-1 vs. TP-3, with lower fold changes and lower statistical significance, but genes markedly similar patterns per gene (Fig. 3B, C, Supplementary Results 1.2, 1.3).

Results are categorized as follows:

1. **DE for *both* DEX treatment AND T1 vs. T3 timecourse progression** (Table 1A, Supplementary Results 1.1,

1.3). 10 genes showed significant DE associated with both DEX exposure *AND* timecourse progression at the T1 vs. T3 timepoint. *Increased* DE genes include the chemokine receptor (CXCR4), Integrin subunit alpha-6 (ITGA6), MAP Kinase 3 (MAPK3), Hepatocyte growth factor receptor (MET), Programmed cell death 4 (PDCD4/neoplastic transformation inhibitor), Phosphatidylinositol 3-kinase regulatory subunit alpha (PIK3R1), Vesicle-associated membrane protein-associated protein A (VAPA), and proto-oncogene tyrosine kinase Yes (YES1).
Decreased expression includes DNA methyltransferase (DNMT3A) and Hypoxanthine-guanine phosphoribosyltransferase (HPRT1).

2. **DE associated with Dex exposure, controlled for time** (Fig. 3A, Table1B, Supplementary Results 1.1). 19 genes showed DE associated with DEX exposure but *not* timecourse progression. *Increased* expression was observed for 13 genes: c-Jun transcription factor (JUN), T-cell specific HMG-box Transcription factor 7-like 2 (TCF7L2), segment-polarity disheveled homolog-1 (DVL1), Epidermal growth-factor receptor (EGFR), Phosphatidylinositol 4,5-bisphostphate 3-kinase catalytic subunit A (PIK3CA), Serine-threonine protein kinase 2 (PAK2), and Wiskott-Aldrich Syndrome protein family member 2 (WASF2).
Decreased expression was seen in lactate dehydrogenase (LDHA, a 'housekeeping' gene candidate), calcium-calmodulin-dependent serine protein kinase 3 (CASK), LIM domain kinase 2 (LIMK2), myosin regulatory light polypeptide 9 (MYL9), Myosin 10 (MYH10), and Lysozyme (LYZ).
3. **DE associated with timecourse, controlled for DEX** (Fig. 3B,C, Table 1C, Supplementary Results 1.3). 25 genes showed DE at TP-3 vs. TP-1 baseline. 14 genes showed *increased* expression, these included Aldehyde dehydrogenase 18, A1 (ALDH18A1), Intestinal alkaline phosphatase 1 (ALPI), Erythrocyte membrane protein band 4.1 (EPB41L3), Integrin AV (ITGAV), Integrin subunit B1 (ITGB1), MAGUK p55 subfamily member 5 (MPP5, palmitoylated membrane protein 5), MAP kinase-kinase 1 (MAP2K1), Myosin light chain kinase (MYLK), NCK-associated protein 1 (NCKAP1), platelet-derived growth factor-C (PDGFC), Phosphatidylinositol-4,5-bisphosphate 3-kinase regulatory subunit 1 (PIK3CB), programmed cell death 4 (PDCD4), and Guanine nucleotide exchange factor, *splice variant 2* (VAV3b).
11 genes showed *decreased* expression over time, these included Kirsten rat sarcoma virus oncogene (KRAS), Occludin (OCLN), Serine/threonine-protein phosphatase 2A (PPP2R1A), Hypoxanthine-guanine phosphoribosyltransferase (HPRT1), diaphanous related formin-3 (DIAPH3), Fibronectin 1 (FN1), dedicator of cytokinesis 1 (DOCK1), cyclin-dependent kinase 4 (CDK4), lymphocyte-homing receptor and cell surface antigen (CD44), Carbonic anhydrase 2 (CA2), and platelet-derived growth factor receptor-beta (PDGFRB).

A trendplot of the 15 highest fold-changed genes (Table 1C, Fig. 3E) shows the progressively increasing fold-changes occurring over time; several genes continue a steady rate of increasing/decreasing expression through T1-T2-T3, while others appear to increase/decrease from T1-T2, with a reduction in rate of differential expression between T2-T3.

The 15 largest fold-changed genes from each experimental comparison (DEX/control) and (TP3/TP1) were chosen, and respective variables applied as classifiers for the PCA analysis (Supplementary Data 1.5). PCA biplot results show that for each tested variable, differential expression constitutes the first principle component, and that the respective variables are explanatory of the majority of variation in expression (71-72%) between differences in DEX/control (Fig. 3D), and TP1/TP3 (Fig. 3E), respectively.

Trans-epithelial electrical resistance (TEER).

TEER was used to quantify epithelial permeability during the DEX timecourse. TEER increased steadily during the timecourse, indicating steadily decreasing permeability as the Caco-2 monolayer forming an increasingly less permeability in both DEX treated and control cell cultures. Between culture days 23-25 however, DEX-treated cultures began to show significantly increased TEER/decreasing permeability relative to control cultures. In control cultures, the rate of permeability decrease levels off, while DEX-treated cultures continue on a steady rate of decreasing permeability (Fig. 5A, Supplementary Results 2). This pattern is consistent with previously reported results of Fischer et al., 2014 (the only other published report of multi-week DEX treatment effect on

epithelial cell culture). Together these datasets indicate that measurable effects of GC on permeability become apparent only after multiple weeks of exposure.

KEGG pathview readouts.

Our KEGG-based pathway selection provide comprehensive pathview readouts for visualizing DE results in the context of canonical pathways of interest (Luo and Brouwer, 2013). Readout of Tight-junction, Regulation of Actin Cytoskeleton (Fig. 5B, C) illustrate that generally, DEX treatment shows less pronounced effects on representative pathways than timecourse-progression (despite correction for confounding variable effects, timecourse DE is partially affected by DEX-enhanced effects). For example, Integrin 6 (ITGA6) expression is increased in both timecourse AND Dex variables (Fig. 4), while the RhoGTPase-pathway gene VAV3b, (guanine nucleotide exchange factor Vav3, *splice variant b*) is increased by timecourse, but not DEX (Table 1B, Fig 5B), and the receptor tyrosine kinase Platelet-derived growth factor receptor B (PDGFRB) expression is strongly decreased during timecourse but not associated with DEX treatment (Table 1C, Fig 5C).

Discussion:

The results provide a pathway-centric point-of-view of differential gene expression as a model for chronic glucocorticoid exposure in the epithelial/enterocyte-like Caco-2 transwell culture system during a 30-day timecourse with three sampling points. Our report provides intestinal epithelial-specific resolution, over weeks rather than hours of exposure rather than hours. Observed co-expression patterns suggest shared inputs from a GC-responsive regulatory network. Here we limit our conclusions on global co-regulatory gene networks and instead discuss observed patterns of co-expression in the context of putative pathway-specific effects in the canonical KEGG tight-junction and Regulation of Actin Cytoskeleton pathways.

Decreased permeability/increased barrier function in 25-day old cultures with 15-days of continuous DEX exposure.

Observation of increasing Trans-epithelial resistance over time indicates decreased permeability over time indicates barrier function becomes increasingly effective in maturing Caco-2 cultures. The trend of increasing TEER continues from initial seeding up to approximately culture day 25 (~Dex-day 15). At this point, TEER in DEX-treated and control cultures become significantly divergent: DEX-treated cultures continue to exhibit increasing TEER/lowered permeability, while in Controls, TEER levels off (Fig. 5A). These results are consistent with Fischer et al. (2014), who independently report the same result. Taken together the two sets of data indicate that physiological effects of DEX exposure on Caco-2 permeability do not appear until at least 20-25 days post-seeding, arguing that longer-term GC exposure may provide protective benefits to intestinal epithelial barrier function. Differential gene expression corresponding with the T3 timepoint may therefore represent time-dependence of GC-associated effects on permeability in Caco-2 monolayers, putatively associated with a phenotypically-responsive expression threshold in genes relevant to permeability.

Occludin (OCLN) shows significantly decreased expression in the T3/T1 comparison, but not under DEX treatment (Fig. 5B), and suggests that DEX treatment opposes time-associated decrease in OCLN expression consistent with observed changes in TEER between treatments (Fig. 5A).

During the timecourse, the enterocyte differentiation marker Carbonic anhydrase 2 (CA2) (Bekku et al, 1998) showed decreased expression, while the colorectal cancer stem marker Aldehyde dehydrogenase 18 A1 (ALDH18A1, Marcato et al, 2011), the pattern is consistent with Caco-2 monolayers having diminished epithelial differentiation, and increasing tendency towards cancer 'stemness' over time.

Dexamethasone-associated differential gene expression.

Although DEX-associated gene expression patterns from the probe panel are relatively less intense than those associated with the time variable, they nonetheless describe a discreet set of DEX-responsive expression, and the overall pattern is consistent with inhibition of expression stress fiber-associated genes and a move toward a

pro-survival mode (Fig. 5,6). DEX-treated cultures exhibit a specific decrease in actomyosin stress-fiber assembly/contraction pathway genes including Myosin 10 (MYH10), its regulator Myosin light-chain regulatory peptide 9 (MYL9), the negative regulator of actin stabilization LIM-domain kinase 2 (LIMK2), and calcium/calmodulin-dependent serine/threonine kinase (CASK, associated with membrane trafficking and centrosome formation) (Fig.5C). The lowered expression indicates putative inhibitory effects on stress-fiber formation and alteration of the cortical actin cytoskeleton.

Lysozyme (LYZ) is a known IBS biomarker showing significantly lower expression in DEX-treated cultures. The physiological significance of LYZ expression in blood is unknown, but in enterocytes may be related to the mucous/sodium flux and microbial dysbiosis associated with stress response.

Dexamethasone carrier molecules may have significant effects. Dexamethasone is not water soluble, so is often compounded with a carrier such as a Cyclodextrin molecule which increases the solubility (and bio-availability), of the Dexamethasone (Tiwari et al, 2010; Muankaew and Loftsson, 2017). Carrier effects are an important consideration in pharmacological design and delivery of water-insoluble molecules such as steroid molecules, and understanding the results of Cyclodextrin:Dexamethasone complexes on tissue models is significant for the understanding pharmacological action (Rodrigues et al, 2014; Davis and Brewster, 2004). Beig et al. (2013) and Fine-Shamier et al. (2017) report cyclodextrin-based formulations to result in decreased permeability, or pericellular transport, of Dex. This is likely the result of the inability of the Cyclodextrin molecule to transit the tight junction, however because of its increased solubility, the bioavailability of Dex to the epithelial cells should remain.

As we did not control for Dexamethasone specifically (i.e,. did not have carrier control), data reported may not be generally interpretable as a fully controlled glucocorticoid treatment. Therefore, results observed for in our experiment must be indicated as the results of Dexamethasone-Cyclodextrin complex.

Our observed, significant divergence of decreased permeability in Dex-treated cultures at ~Day 21-25, is similar to the result of Fischer et al. (2014), who also used a “carrier minus Dex” control. It is common practice in cell-culture experiments with Dex, to add carrier without Dex in order to control for nonspecific effects of the carrier itself. Our statistical support shows that differential expression results are valid, these data are therefore useful for interpretation of both Dex and Dex-Cyclodextrin effects.

Complementary patterns of Dexamethasone *and* timecourse-associated DE in a subset of panel genes.
For each variable (DEX/Control, T3/T1), DE analysis was performed under correction for the opposite confounding variable, respectively. Yet, 10 genes had significant differential expression for *both* DEX and TP3 vs. TP1 tests (Table 1A, Fig. 4). Chemokine receptor (CXCR4), Programmed cell death 4 (PDCD4), and Hepatocyte growth factor receptor (MET), each exhibit increased DEX-associated expression and increased expression at each progressive at each timepoint. Other genes show similar expression between DEX vs Control at TP1, but DE becomes increasingly significant at TP2 and TP3; these include Vesicle-associated membrane protein A (VAPA), phosphatidylinositol-3-kinase (PIK3R1), and Integrin alpha subunit 6 (ITGA6). Two genes show *decreased* expression for both variables including a DNA methyltransferase (DMNT3A) and a guanine phosphoribosyltransferase (HPRT1). For these 10 genes, DEX treatment apparently *enhances* trends occurring during timecourse progression. (Figs. 4, 5, 6)

It has been observed that GC synthesis can take place *in the intestinal epithelia* (25, 32); a possible explanation for our observe pattern is therefore that Caco-2 cells themselves produce endogenous GC affecting gene expression over time, with DEX treatment enhancing already-active GC response. We undertook rigorous adherence to best cell culture practices, nonetheless these observed responses may also represent unknown/uncontrolled culture variables.

ITGA6, PI3KR1, MAPK3 genes showed differential expression in this category. These canonical members of RhoGTPase and PIK3/Akt -pathways are central players in actin cytoskeleton, focal adhesion, cell polarity and stress-fiber regulatory pathways (Iden and Collard, 2008). Significant upregulation of all 3 show that a general increase pathway activity, or at least an increased pathway *potential* may result from increased presence of these gene products.

Chemokine receptor CXCR4 (aka. CD184, *fusin*) is known as a T-cell HIV receptor and a leukocyte-associated transendothelial migration receptor, also playing an important role in epithelial polarity during the endometrial implantation window. CXCR4 expression is largely localized to immune cells and lymphoid tissue, however was included in our codeset to test possible epithelial-specific responsiveness and expression as putative GI stress-associated biomarkers (Abey et al, 2016). We observe CXCR4 expressed at low relative levels in Caco-2 cells, however exhibiting a high fold change for both experimental variables.

DEX-associated increase in expression of the pro-survival JUN transcription factor is interesting in light of previous that GCR/AP-1 promotor binding suppresses JUN transcription (Wei et al, 1998); this may be a phenomenon resulting from adenocarcinoma-specific alterations present in the cell line. However, DEX-associated, *ras*-dependent stimulation of c-Jun expression in the rat intestinal epithelial cell line IEC-6 was reported by Boudreau et al. (1999), providing some indication that DEX-associated c-Jun activation may potentially be an intestinal-epithelial specific response.

Differential expression of tyrosine kinase growth factor receptors (RTK).
Differential expression observed in the various growth factor receptor tyrosine kinases (RTKs) tested (Fig. 6B, Supplementary Results) indicate that over time and in response to DEX exposure, cells may become differentially sensitive to different growth factors. The most pronounced fold change is seen in decreased expression of platelet-derived growth factor receptor B (PDGFRB) at TP3. Fibroblast growth factor receptor (FGFR) gene expression also decreases at TP3, while both DEX and TP3 exhibit increased expression of Hepatocyte growth factor receptor (MET). DEX-specific increase in epidermal growth factor (EGFR) is also observed.

Toward a systems-level understanding of transcriptional and physiological response.
A major goal of modern molecular and cellular biology is to develop systems-level representation of biological processes in a manner which facilitates clear and concise interpretation. Here we seek to provide a readout of differential transcription in an intestinal epithelial model, and to provide an evaluation of transcriptional effects of glucocorticoid exposure over long time periods for pathways related to barrier function and permeability. Global transcriptional effects have not been observed in these experiments, and readout does not provide a view of translation/protein expression outcomes, underlying transcription-factor binding and trans-activation/trans-repression and co-regulatory interactions (although some may be inferred). Results from the use of a single cell-line may not be generalizable for all observations, and *in-vivo* cellular physiology is highly influenced by signaling and interaction with surrounding cells and tissues not present in cellular monocultures.

References

1. **Abey SK, et al.** Lysozyme association with circulating RNA, extracellular vesicles, and chronic stress. *BBA Clinical* 7:23-25, 2016.
2. **Appenstrom P.** The Rho GTPases Have Multiple Effects on the Actin Cytoskeleton. *Experimental Cell Research* 246:20-25, 1999.
3. **Beig A, Agbaria R, Dahan A.** Oral delivery of lipophilic drugs: the tradeoff between solubility increase and permeability decrease when using cyclodextrin-based formulations. *PLoS One* 8(7):e68237, 2013.
4. **Benjamini Y, Yekutieli D.** The control of the false discovery rate in multiple testing under dependency. *Ann. Statist* 29(4):1165-1188, 2001.

5. **Bekku S, et al.** Carbonic anhydrase I and II as a differentiation marker of human and rat colonic enterocytes. *Res Exp Med* 198:175-185, 1998.
6. **Blume LF, Denker M, Gieseler F, Kunze T.** Temperature corrected transepithelial electrical resistance (TEER) measurement to quantify rapid changes in paracellular permeability *Parmazie* 65(1):19-24, 2010.
7. **Boivin MA, et al.** Mechanism of glucocorticoid regulation of the intestinal tight junction barrier. Am J *Physiol Gastrointest Liver Physiol* 292:G590-G598, 2007.
8. **Boudreau F, et al.** Negative regulation of glucocorticoid-dependent induction of c-fos by ras in intestinal epithelial cells. *Mol Cell Biochem* 195(1-2):9-111, 1999.
9. **Bruewer, M., et al.** RhoA, Rac1, and Cdc42 exert distinct effects on epithelial barrier via selective structural and biochemical modulation of junctional proteins and F-actin. *Am J Physiol Cell Physiol* 287:C327-C335, 2004.
10. **Burridge K, Wennerberg K.** Rho and Rac Take Center Stage. *Cell* 116:167-179, 2004.
11. **Buttgereit F, et al.** Optimised glucocorticoid therapy: the sharpening of an old spear. *The Lancet*. 365(9461):801-803, 2005.
12. **Cain DW, Cidlowski JA.** Immune regulation by glucocorticoids. *Nature Reviews Immunology*. 17:233-247, 2017.
13. **Citi, S., et al.** Epithelial junctions and Rho family GTPases: the zonular signalsome. *Small GTPases* 5(4):e973960, 2014.
14. **Chinenov Y, et al.** Glucocorticoid receptor coordinates transcription factor-dominated regulatory network in macrophages. *BMC Genomics* 15:656, 2014.
15. **Coutinho AE, Chapman KE.** The anti-inflammatory and immunosuppressive effects of glucocorticoids, recent developments and mechanistic insights. *Molecular and Cellular Endocrinology* 335(1):2-13, 2011.
16. **Davis ME, Brewster ME.** Cyclodextrin-based pharmaceutics: past, present and future. *Nat Rev Drug Discov* 3(12):1023-35, 2004.
17. **Dorfel MJ, Huber O.** Modulation of Tight Junction Structure and Function by Kinases and Phosphatases Targeting Occludin *Journal of Biomedicine and Biotechnology*, 2012.
18. **Fine-Shamir N, Beig A, Zur M, Lindley D, Miller JM, Dahan A.** Toward Successful Cyclodextrin Based Solubility-Enabling Formulations for Oral Delivery of Lipophilic Drugs: Solubility-Permeability Trade-Off, Biorelevant Dissolution, and the Unsteirred Water Layer *Molecular pharmaceutics* 14(6):2138-2146, 2017.
19. **Fischer A, et al.** Glucocorticoids regulate barrier function and claudin expression in intestinal epithelial cells via MKP-1. *Am J Physiol Gastrointest Liver Physiol* 306:G218-G228, 2014.
20. **Geiss GK, et al.** Direct multiplexed measurement of gene expression with color-coded probe pairs. *Nature Biotechnology* 26:317-325, 2008.
21. **Gerber AN.** Glucocorticoids and the Lung. *Adv Exp Med Biol*. 872:279-98, 2015.
22. **Gonzalez-Mariscal L, Tapia R, Chamorro D.** Crosstalk of tight junction components with signaling pathways. *Biochimica et Biophysica Acta* 1778:729-756, 2008.
23. **Gupte R, et al**. Glucocorticoid receptor represses proinflammatory genes at distinct steps of the transcription cycle. *PNAS* 110(36):14616-14621, 2013.
24. **Hidalgo IJ, Raub TJ, Borchardt, RT.** Characterization of the Human Colon Carcinoma Cell Line (Caco-2) as a Model System for Intestinal Epithelial Permeability. *Gastroenterology* 96:736-49, 1989.
25. **Iden S, Collard JG.** Crosstalk between small GTPases and polarity proteins in cell polarization. *Nature Reviews Molecular Cell Biology* 9:846-859, 2008.
26. **Kadmiel M, Cidlowski JA.** Glucocorticoid receptor signaling in health and disease. *Trends in pharmacological sciences* 34(9):518-530, 2013.
27. **Kanehisa M, et al.** KEGG: Kyoto Encyclopedia of Genes and Genomes. *Nucleic Acids Res* 30, 2000.
28. **Kostadinova F, Schwaderer J, Sebeo V, Brunner T.** Why does the gut synthesize glucocorticoids?. *Annals of Medicine* 46(7):490-7, 2014.
29. **Krug, SM, Schulzke J., Fromm M.** Tight junction, selective permeability, and related diseases. *Seminars in Cell & Developmental Biology* 36:166-176, 2014.
30. **Lee SH.** Intestinal Permeability Regulation by Tight Junction: Implication on Inflammatory Bowel Diseases.

Intestinal Research 13(1):11-18, 2014.
31. **Luo W, Brouwer C.** Pathview: an R/Bioconductor package for pathway-based data integration and visualization. *Bioinformatics* 29(14):1830-1831, 2013.
32. **Mack NA, Georgiou M.** The interdependence of the Rho GTPases and apicobasal cell polarity. *Small GTPases* 5(2):e973768, 2014.
33. **Marcato P, Dean CA, Ciacomantoinio CA, Lee PW.** Aldehyde dehydrogenase: its role as a cancer stem cell marker comes down to the specific isoform. *Cell Cycle* 10(9):1378-84, 2011.
34. **Muankaew C, Loftsson T.** Cyclodextrin-Based Formulations: A Non-Invasive Platform for Targeted Drug Delivery. *Basic & Clinical Pharmacology & Toxicology* 122(1), 2017.
35. **Natoli M, Bruno DL, D'Agnano I, Zucco F, Felsani A.** Good Caco-2 cell culture practices. *Toxicology in Vitro* 26:1243-1246, 2012.
36. **Noti M, Sidler D, Brunner T.** Extra-adrenal glucocorticoid synthesis in the intestinal epithelium: more than a drop in the ocean? *Semin Immunopathol*. 31(2):237-48, 2009.
37. **Perkins JR, et al.** ReadqPCR and NormqPCR: R packages for the reading, quality checking and normalization of RT-qPCR quantification cycle (Cq) data. *BMC Genomics* 13:296, 2012.
38. **Petta I, et al**. The Interactome of the Glucocorticoid Receptor and Its Influence on the Actions of Glucocorticoids in Combatting Inflammatory and Infectious Diseases. *Microbiology and Molecular Biology Reviews* 80(2):495-522, 2016.
39. **Robinson JM**, **Henderson W.** Modelling the structure of a ceRNA-theoretical, bipartite microRNA-mRNA interaction network regulating intestinal epithelial cellular pathways using R programming. *BMC Res Notes* 11(1):19, 2018.
40. **Rodrigues PO, et al.** Pharmacodynamic and Pharmacokinetic Studies of B-Cyclodextrin:Dexamethasone Actate Complexes in Mice. *Brazilian Archives of Biology and Technology* 57(6):887-894, 2014.
41. **Schneeberger EE, Lynch RD.** The tight junction: a multifunctional complex. *Am J Physiol Cell Physio*l 286:C1213-C1228, 2004.
42. **Soderholm JD, Perdue MH.** Stress and the Gastrointestinal Tract II. Stress and intestinal barrier function. *Am J Physiol Gastrointest Liver Physiol*. 280:G7-G13, 2001.
43. **Tiwari G, Tiwari R, Rai AK.** Cyclodextrins in delivery systems: Applications. *J Pharm Bioallied Sci* 2(2):72-79, 2010.
44. **Turner JR, et al.** The role of molecular remodeling in differential regulation of tight junction permeability *Semin Cell Dev Biol*, 2014.
45. **Quiros M, Nusrat A.** RhoGTPases, actomyosin signaling and regulation of the epithelial Apical Junctional Complex. *Seminars in Cell & Developmental Biology* 36:194-203, 2014.
46. **Uhlen M, et al.** Tissue-based map of the human proteome. *Science* 347(6220), 2015.
47. **Uhlenhaut NH, et al.** Insights into Negative Regulation by the Glucocorticoid Receptor from Genome-Wide Profiling of Inflammatory Cistromes. *Mol Cell* 49(1):158-171, 2013.
48. **Vandesompele J. et al.** Accurate normalization of real-time quantitative RT-PCR data by geometric averaging of multiple internal control genes. *Genome Biology* 3(7):RESEARCH0034, 2002.
49. **Vockley, et al.** Direct GR Binding Sites Potentiate Clusters of TF Binding across the Human Genome. *Cell* 166, 1269-81, 2016.
50. **Wei P, Inamdar N, Vedeckis WV.** Transrepression of c-jun gene expresson by the glucocorticoid receptor requires both AP-1 sites in the c-jun promoter. *Mol Endocrinol*. 12(9):1322-33, 1998.
51. **Xavier AM, et al.** Gene Expression Control by Glucocorticoid Receptors during Innate Immune Responses. *Frontiers in Endocrinology* 7:31, 2016.
52. **Zihni C, Mills C, Matter K, Balda MS.** Tight junctions: from simple barriers to multifunctional molecular gates. *Nature Reviews Molecular Cell Biology*. 17:564-580, 2016. www.proteinatlas.org.

Figure Captions

Figure 1. The epithelial tight junction regulates permeability in Caco-2 cell line and intestinal enterocyte

monolayers. **A.** Laser-scanning confocal microscopy (LSCM) with immunofluorescent staining of Occludin and ZO-1 in polarized Caco-2 monolayer shows intracellular interaction of the major tight junction components facilitating the epithelial barrier in the cellular epithelial membrane. **B.** Complex protein structure of the tight junction and its interaction with the actin bands of the cortical actin cytoskeleton of polarized epithelia. **C.** Actin cytoskeleton regulatory pathways downstream of growth factor receptor tyrosine kinases, integrins, and cytokine activation G-protein coupled receptors include RhoGTPase, MAP kinase, and PI3K-Akt signaling which affect actin stress-fiber polymerization and actomyosin assembly and contraction affecting the stabilized cortical actin cytoskeleton and interaction with the tight junction.

Figure 2. Caco-2 transwell system and experimental timeline. **A.** Trans-epithelial electrical resistance (TEER) measured in permeable-membrane culture system used in this experiment provides a physiological readout for epithelial barrier function. **B.** Dexamethasone was included in culture media after a 12-day period of maturation and polarization of monolayer. RNA was extracted at 3 timepoints after initial addition of DEX and terminal 30-culture days with 14 days of continuous DEX exposure.

Figure 3. Differential expression and PCA analysis. **A.** Volcano plots showing DGE results for Dex vs. Control comparison. **B.** Volcano plots showing DGE results for T2 vs. T1 and T3 vs. T1 timepoints. **C.** Principle components analysis results for the top DEX-associated differentially expressed genes indicates DEX treatment explains ~72% of variation in expression of these genes. **D.** Principle components analysis results for the top T3 vs. T1-associated differentially expressed genes indicates timepoint effects explain ~72% of variation in expression of these genes, with a trendplot showing relative expression differences by timepoint.

Figure 4. Differentially expressed genes significant for both DEX and Timepoint. The violin plots show expression by log2(count) for each gene, at each experimental sampling point, showing how expression affected similarly by DEX exposure produces an enhancement of trends observed over timecourse progression.

Figure 5. Dex- and timecourse-associated effects on transcription and permeability. **A.** Graph of TEER measurements independently confirms observations of Fischer et al., 2014, showing a delayed effect of DEX on permeability appearing to become significant at or about culture day 25. **B.** KEGG Pathview readouts indicate differential gene expression in the canonical tight junction pathway, *specifically* decreased expression of Occludin over time.

Figure 6. KEGG pathview for regulation of actin cytoskeleton pathway and RTKs. **A.** Pronounced changes of timecourse-associated expression observed in canonical PI3K pathway and integrin pathway. **B.** Differential expression of growth factor receptors. **C.** Differential expression in actomyosin assembly and contraction components.

Table 1. Differential Gene Expression by Treatment at FDR ≤ .05. Differentially expressed genes by treatment, with full gene name and canonical KEGG pathway associations. Bottom shows a list of top canonical KEGG pathways represented in the complete gene set.

Author Contributions:

Robinson designed the experiments, conceived and designed the custom Nanostring codeset, performed cell culture activities, collected confocal image data, collected TEER data, performed RNA extractions, performed Nanostring protocols and operated the nCounter instrument for each replicate, on-site at the Henderson lab-NINR. Robinson performed statistical and bioinformatic analyses using the R-based nSolver 3.0 software package, and TEER data analysis using R/R-Studio. Robinson wrote and revised the original text and produced

figures (see acknowledgements for additional Figure 1 and 2 contributions).

Abey designed the experiments, set up laboratory infrastructure for cell culture experiments, contributed to Nanostring codeset design and content, collected and analyzed data and performed cell culture tasks.

Kenea performed cell culture tasks.

Henderson designed the experiments, contributed to the Nanostring codeset design and content, organized and supervised research and administration, edited and revised the manuscript.

Figures

Figure 1. The epithelial tight junction regulates permeability in Caco-2 cell line and intestinal enterocyte monolayers.

A. LSCM image with Occludin (OCLN, *green*) and Zona Occludens-1 (TJP, *red*) in polarized Caco-2 monolayer. Top-down (left) and oblique (right) view of the same z-stack.

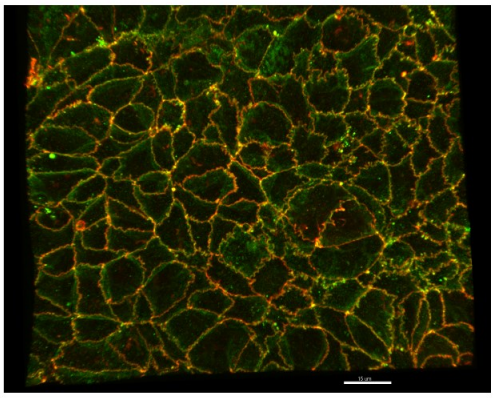

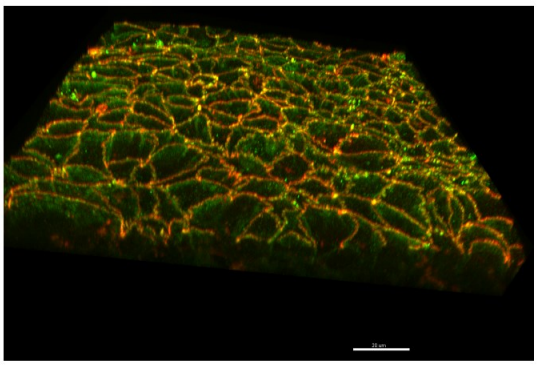

B. The tight-junction protein complex facilitates selective permeability and interacts with the actin cytoskeleton.

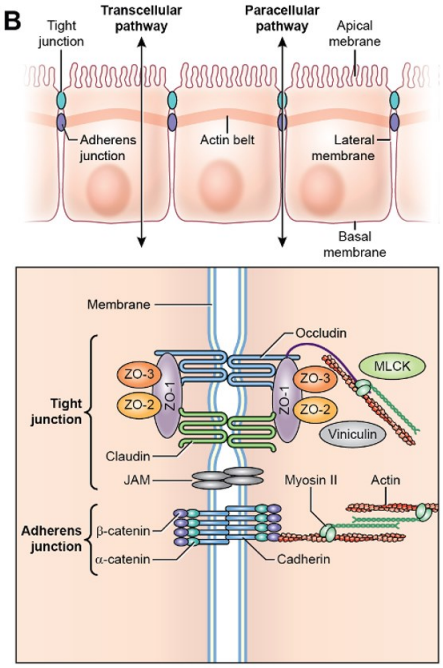

C. Upstream regulation by the RhoGTPase pathway serves to integrate signalling by integrins, growth factor receptors with actin cytoskeletal responses.

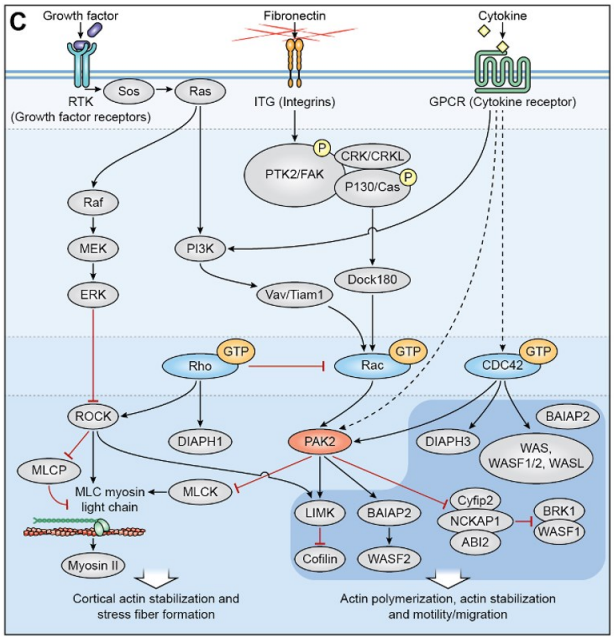

Figure 2. Caco-2 transwell culture system and experimental timeline.

A Permeability of Caco-2 polarized monolayer cultures quantified using transepithelial resistance (TEER)

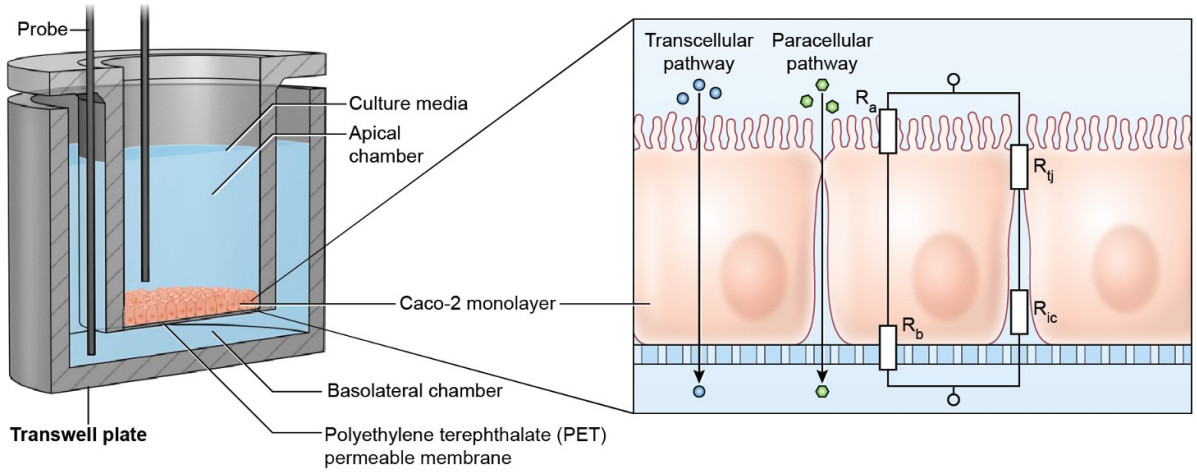

B RNA was extracted at three experimental timepoints, each for Control and DEX-treated monolayers

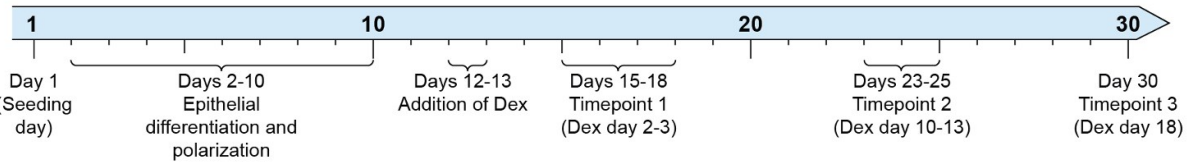

Figure 3. Differential Expression and PCA Analysis

A. DEX-associated DE

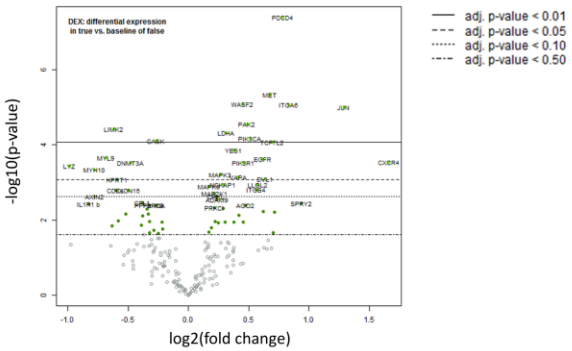

B. Timeline-associated DE

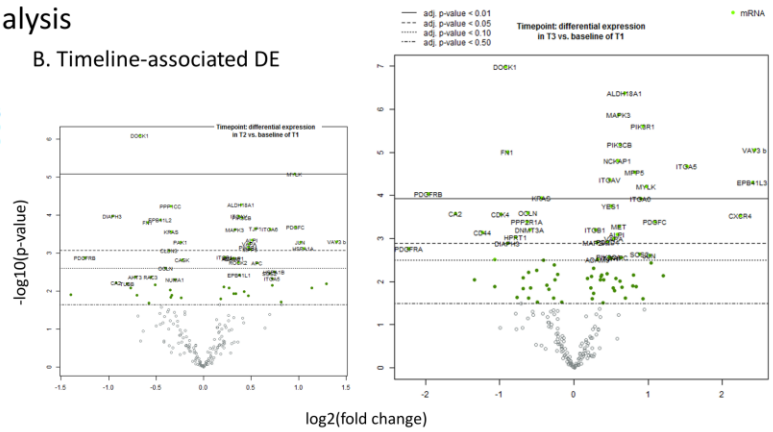

C. PCA, DEX-associated DE genes

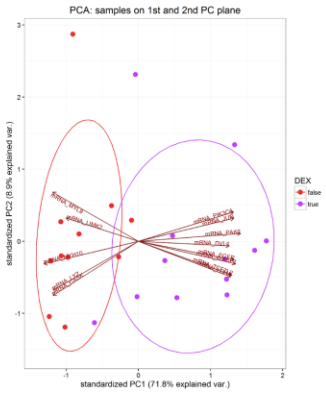

D. PCA, Timeline-associated DE genes

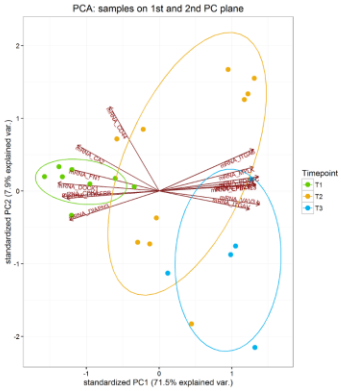

E. Trendplot Indicates Time-Associated Differential Expression

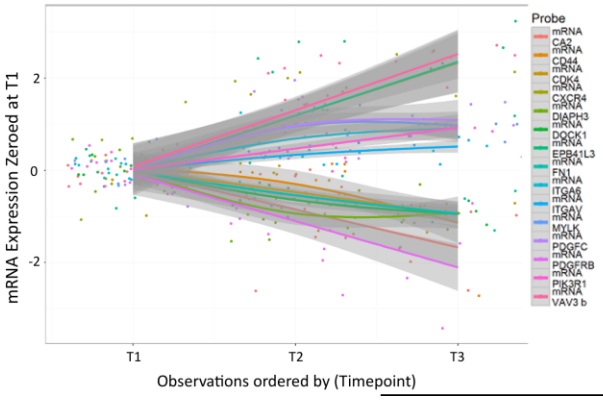

Figure 4. Differentially Expressed Genes Significant for Both Time and DEX treatment

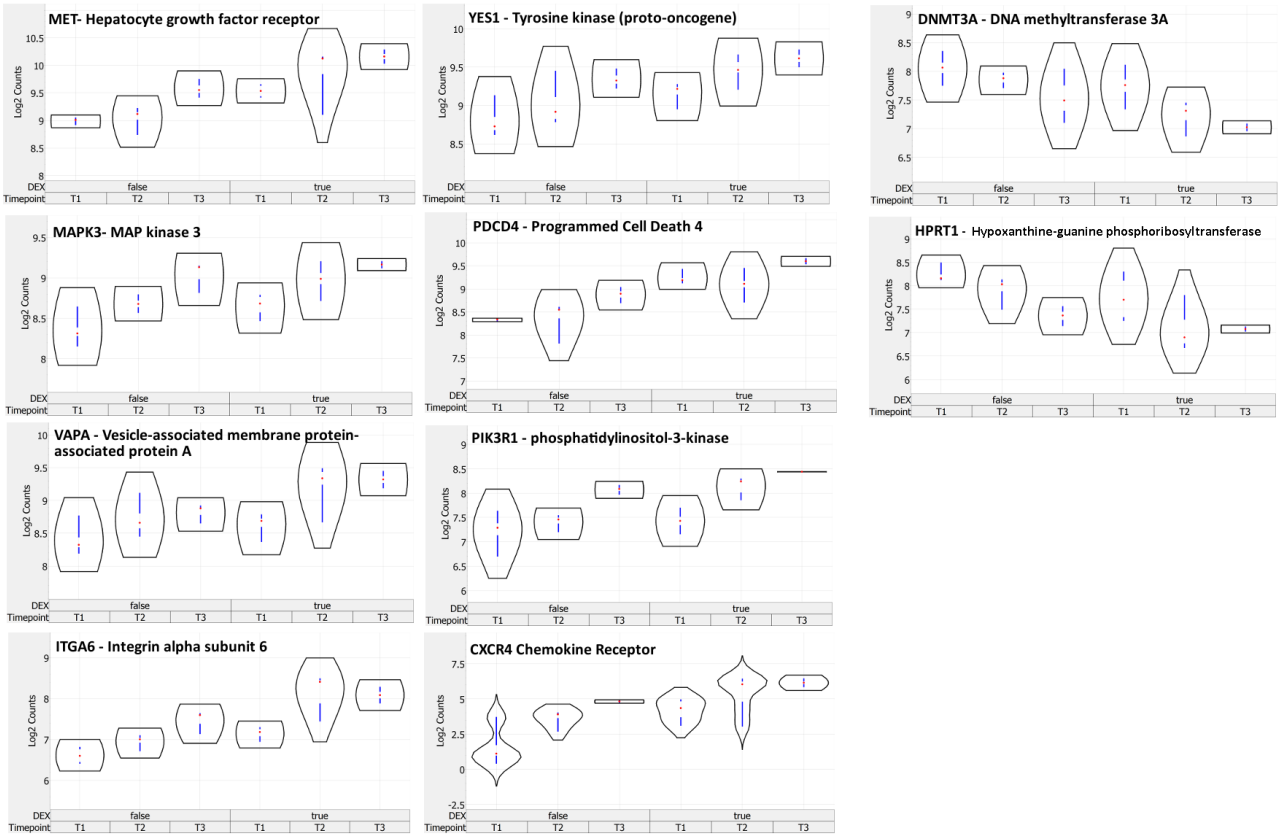

Figure 5. DEX and timecourse-associated effects on transcription and permeability

A. DEX affects Caco-2 permeability after extended treatment

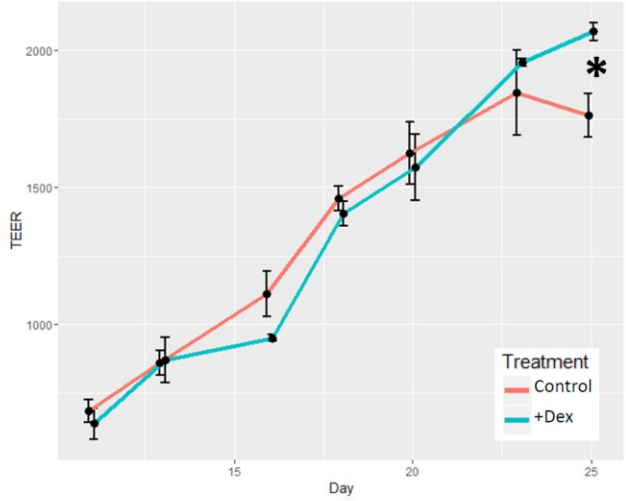

B. Cell-culture longevity is associated with lower expression of differentiation markers.

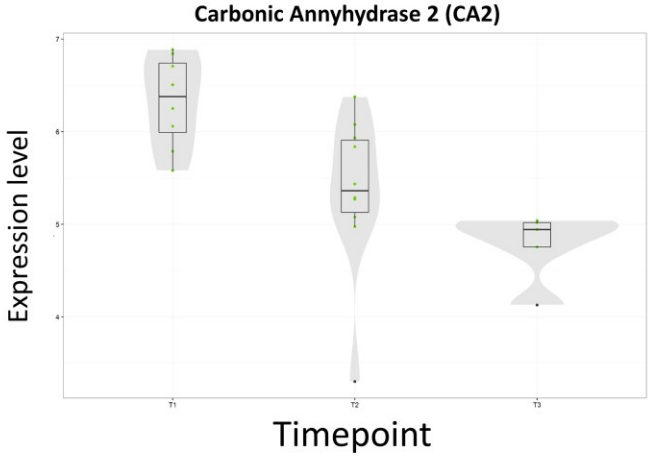

C. DEX and Timecourse-specific DE in the KEGG Tight Junction Pathway.

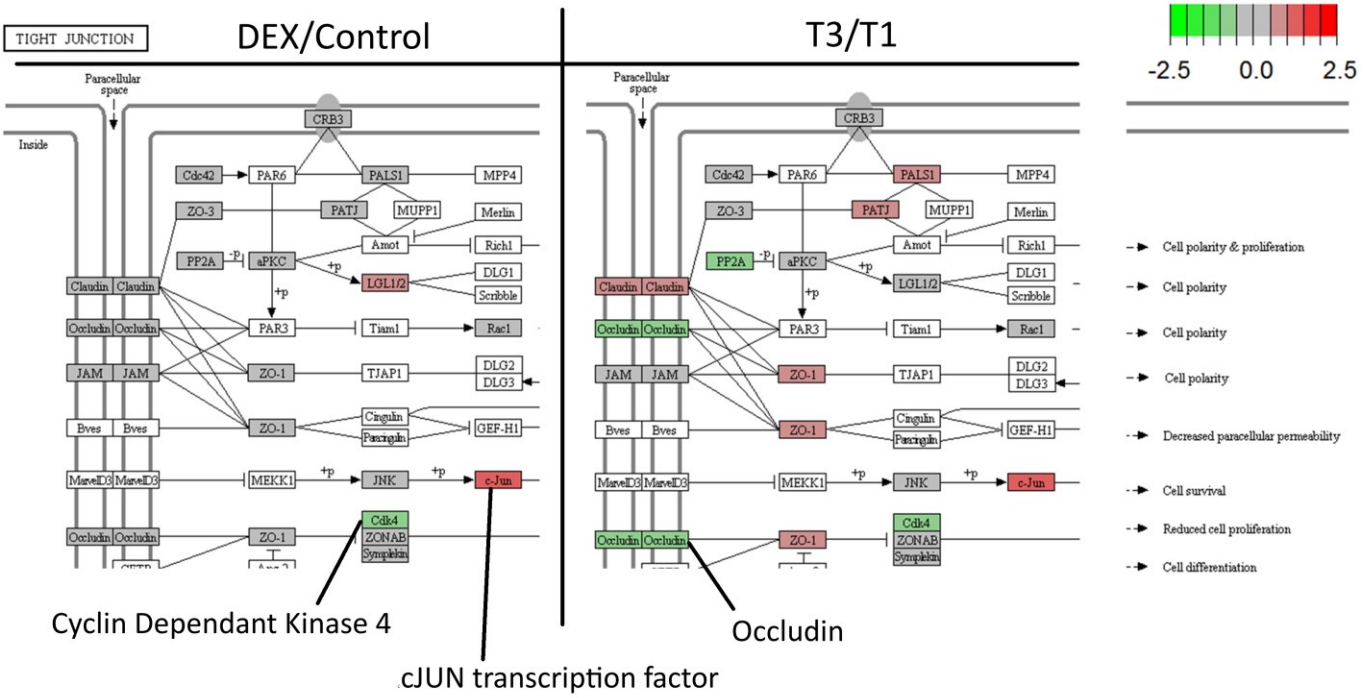

Figure 6. KEGG Pathview for Regulation of Actin Cytoskeleton Pathwayand RTKs

A. GTPase Signal Transduction Pathway DE

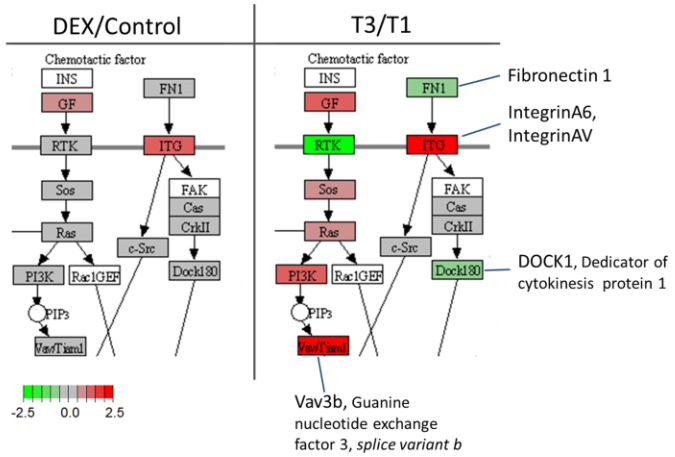

B. Growth Factor/ Receptor Tyrosine Kinase DE

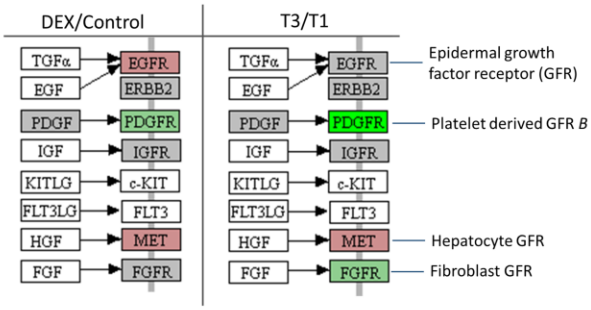

C. Actomyosin Assembly Regulation(KEGG Pathview).

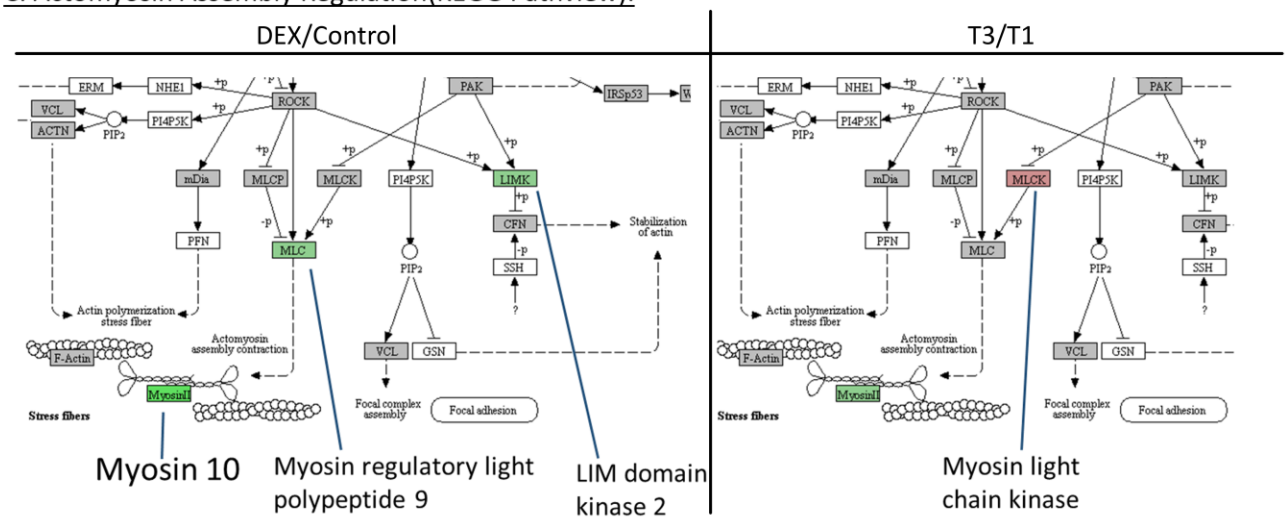

Table 1. Differential Expression by Variable (FDR <= .05)

DE for both (DEX) and (T3vT1) variables

GeneID	Gene Description	fold change (DEX)	BY.p.value (DEX)	fold change (T3vs T1)	BY.p.value (T3vs T1)	TJ	AC	CRC	FA	AJ	Additional Associations
CXCR4-mRNA	C-X-C chemokine receptor type 4	3.16	0.021	4.72	0.017						IBS-associated differential expression (Abey et al. 2017)
ITGA6-mRNA	integrin subunit alpha-6	1.78	0.002	1.87	0.009		X		X		
PDCD4-mRNA	programmed cell death 4 (neoplastic transformation inhibitor)	1.72	4.91e-05	1.37	0.047						CRC-associated miRNA target
MET-mRNA	hepatocyte growth factor receptor	1.60	0.002	1.52	0.026						CRC-associated miRNA target
PIK3R1-mRNA	Phosphatidylinositol 3-kinase	1.37	0.021	1.90	1.4e-06		X	X	X		
VAPA-mRNA	VAMP (vesicle-associated membrane protein)-associated protein A	1.33	0.041	1.45	0.041	X					
YES1-mRNA	Proto-oncogene tyrosine-protein kinase Yes	1.30	0.014	1.42	0.012	X				X	
MAPK3-mRNA	Mitogen-activated protein kinase 3	1.20	0.038	1.20	0.038		X	X	X	X	
DNMT3A-mRNA	DNA (cytosine-5)-methyltransferase 3A	0.72	0.021	0.66	0.029						CRC-associated miRNA target
HPRT1-mRNA	hypoxanthine phosphoribosyltransferase 1	0.66	0.044	0.58	0.039						Reference gene candidate

DEX-specific DE

GeneID	Gene Description	fold change	BY.p.value	TJ	AC	CRC	FA	AJ	Additional Associations
JUN-mRNA	c-Jun transcription factor	2.45	0.002	X	X	X			Wnt pathway
TCF7L2-mRNA	Transcription factor 7-like 2(T-cell specific, HMG-box)	1.62	0.009			X		X	Wnt pathway
DVL1-mRNA	dishevelled segment polarity protein 1	1.55	0.044						Wnt, Notch pathways
EGFR-mRNA	Epidermal growth factor receptor	1.53	0.021		X		X	X	
PIK3CA-mRNA	Phosphatidylinositol 4,5 bisphosphate 3-kinase, catalytic subunit A	1.43	0.009		X	X	X		
PAK2-mRNA	Serine-threonine protein kinase 2	1.40	0.006		X		X		
WASF2-mRNA	WAS protein family, member 2	1.37	0.002		X			X	
LDHA-mRNA	Lactase dehydrogenase A	1.24	0.007						Candidate reference gene
CASK-mRNA	calcium/calmodulin-dependent serine protein kinase (MAGUK family)	0.83	0.009	X					
LIMK2-mRNA	LIM domain kinase 2	0.65	0.007	X					Rac-Rock-Rho pathway (Burridge&Wennerberg, 2004)
MYL9-mRNA	Myosin regulatory light polypeptide 9	0.62	0.021		X				
MYH10-mRNA	Myosin 10	0.58	0.029	X	X				
LYZ-mRNA	Lysozyme	0.50	0.024						IBS-associated differential expression (Abey et al. 2017)

T3vT1-specific DE

GeneID	Gene Description	fold change	BY.p.value	TJ	AC	CRC	FA	AJ	Additional Associations
VAV3 b-mRNA	vav 3 guanine nucleotide exchange factor, splice variant 2	5.39	0.002		X		X		
EPB41L3-mRNA	erythrocyte membrane protein band 4.1	5.31	0.005	X					
ITGAV-mRNA	integrin, alpha V	2.87	0.003		X		X		
PDGFC-mRNA	platelet derived growth factor C	2.13	0.021		X		X		
MYLK-mRNA	myosin light chain kinase	1.96	0.006		X		X		
DIAPH3-mRNA	diaphanous-related formin 3	0.54	0.047						Rac-Rock-Rho pathway (Burridge&Wennerberg, 2004)
FN1-mRNA	Fibronectin 1	0.54	0.002		X		X		
DOCK1-mRNA	dedicator of cytokinesis 1	0.53	0.000		X		X		
CDK4-mRNA	cyclin dependent kinase 4	0.51	0.016	X					
CD44-mRNA	CD44 molecule (Indian blood group)	0.43	0.033						CRC-cancer stem marker
CA2-mRNA	carbonic anhydrase 2	0.33	0.016						Histological enterocyte differentiation marker
PDGFRB-mRNA	platelet-derived growth factor receptor, beta polypeptide	0.26	0.006		X		X		

TOP 20 Pathways Represented by Codeset Panel (KEGGPATH analysis)

1. Regulation of actin cytoskeleton (**AC**)
2. Focal adhesion (**FA**)
3. Tight junction (**TJ**)
4. Pathways in cancer
5. Proteoglycans in cancer
6. PI3K-Akt signaling pathway
7. Rap1 signaling pathway
8. Leukocyte transendothelial migration
9. MAPK signaling pathway
10. Chemokine signaling pathway
11. Ras signaling pathway
12. HTLV-I infection
13. Adherens junction (**AJ**)
14. Colorectal cancer (**CRC**)
15. cAMP signaling pathway
16. Sphingolipid signaling pathway
17. Prostate cancer
18. MicroRNAs in cancer
19. Hepatitis C
20. Wnt signaling pathway

Supplementary Methods 1. Tab 1 – Probe annotations (ie. KEGG pathway membership). Tab2 – Probe sequence and accession details. Tab3 – Results of geNorm reference gene selection, showing reference genes selected by variance after normalization.

Supplementary Results 1 – Differential Expression (fold change and P-value) for Dex/Control (tab 1), T2/T1 (tab 2), and T3/T1 (tab 3), and an extended version of Table 1 with replicate design (tab 4).

Acknowledgements.
Research reported in this publication was supported by the U.S. Department of Health and Human Services, National Institutes of Health, National Institute of Nursing Research, Division of Intramural Research to Wendy A. Henderson, 1Z1ANR000018-01-8; Intramural Research Training Awards to Jeffrey M. Robinson, Sarah K. Abey, and Natnael D. Kenea. The content is solely the responsibility of the authors and does not necessarily represent the official views of the National Institutes of Health.

Authors acknowledge:
-**Ethan Tyler** of the NIH Medical Arts Division for his graphic design work on Fig.1 B,C, and Fig. 2.
-**Dr. Christian Combs** at the NIH National Heart Lung and Blood Institute microscopy core for help and guidance in collecting the confocal images presented in Fig. 1A.

-**Dr. Greg Gonye** (formerly at Nanostring Technologies) for his facilitation for the Nanostring nCounter® device.

Current addresses for co-authors:
Dr. Sarah Abey. skabey1@gmail.com
Mr. Natnael Kenea. knatnael@gmail.com

Disclosures. Robinson currently holds one short-term Nanostring Technologies options contract (exp. 7/20/18).